Chapter 4

Muon spectrometer

Muon detection is performed in the pseudo-rapidity region $-4.0 < \eta < -2.5$ by the muon spectrometer. With this detector, the complete spectrum of heavy-quark vector-mesons reasonances (i.e. J/ψ, ψ', Υ, Υ' and Υ''), as well as the ϕ meson, will be measured in the $\mu^+\mu^-$ decay channel. The simultaneous measurement of all the quarkonia species with the same apparatus will allow a direct comparison of their production rate as a function of different parameters such as transverse momentum and collision centrality. In addition to vector mesons, the unlike-sign dimuon continuum up to masses around 10 GeV/c^2 will be measured. Since at LHC energies the continuum is expected to be dominated by muons from the semi-leptonic decay of open charm and open beauty, it will be possible to study the production of open (heavy) flavours with the muon spectrometer. Heavy-flavour production in the region $-2.5 < \eta < -1$ will be accessible through measurement of $e-\mu$ coincidences, where the muon is detected by the muon spectrometer and the electron by the TRD.

The muon spectrometer will participate in the general ALICE data taking for Pb-Pb collisions at luminosity $\mathscr{L} = 10^{27}\,\mathrm{cm}^{-2}\mathrm{s}^{-1}$. The situation is different for intermediate-mass ion collisions (e.g. Ar-Ar). In this case, beside a general ALICE run at low luminosity, $\mathscr{L} = 10^{27}\,\mathrm{cm}^{-2}\mathrm{s}^{-1}$, to match the TPC rate capability, a high-luminosity run at $\mathscr{L} = 10^{29}\,\mathrm{cm}^{-2}\mathrm{s}^{-1}$ is also foreseen, to improve the Υ counting statistics. For the high-luminosity run, the muon spectrometer will take data together with a limited number of ALICE detectors (ZDC, SPD, PMD, T0, V0 and FMD) able to sustain the event rate. These detectors allow the determination of the collision centrality.

4.1 Design considerations

The main design criteria of the spectrometer were driven by the following considerations:

As the accuracy of dimuon measurements is statistics limited (at least for the Υ family), the spectrometer's geometrical acceptance was chosen as large as possible. In addition, a large acceptance down to zero p_{t} is required for measuring direct J/ψ production. At high p_{t} a large fraction of J/ψ's is produced via b-decay [136]; based on Tevatron measurements [137] the contribution from b-decay to the total J/Ψ yield is $\approx 10\%$ for $p_{\mathrm{t}} < 3-4\,\mathrm{GeV}/c$ and then it increases linearly to $\approx$ 40% for p_{t} around $15-18\,\mathrm{GeV}/c$. Since muon identification in the heavy-ion environment is only feasible for muon momenta above about 4 GeV/c because of the large amount of material

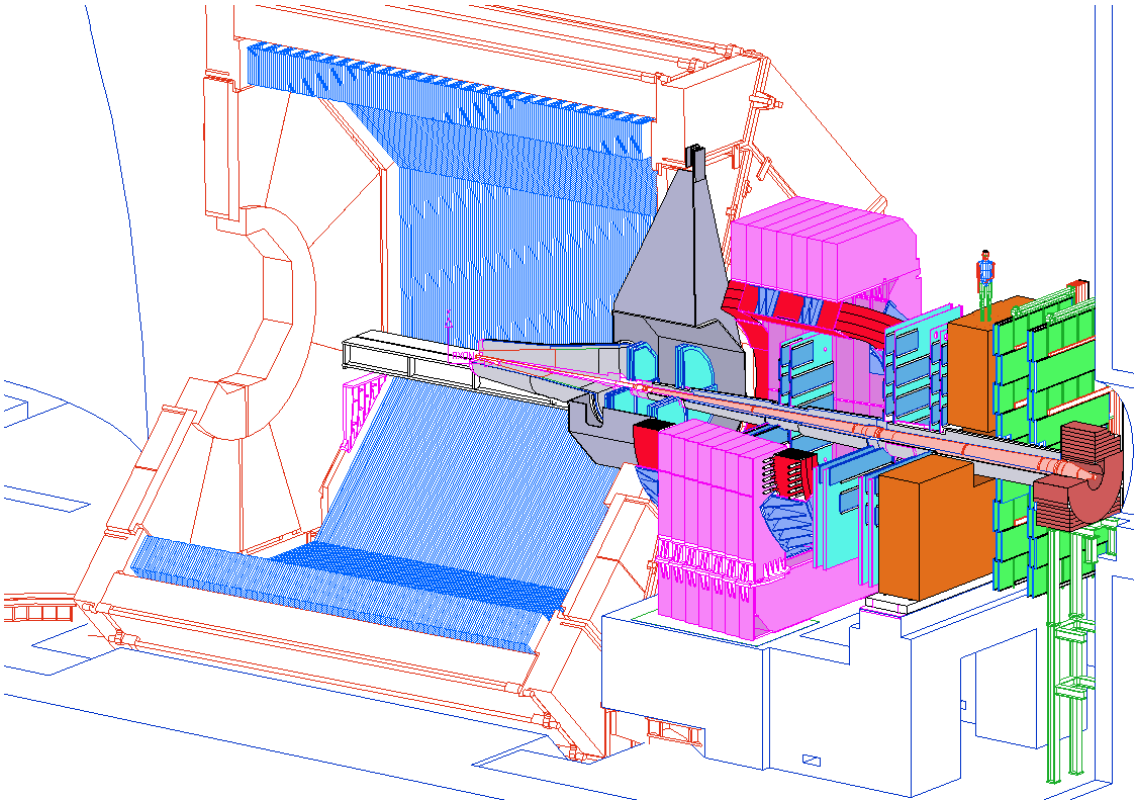

Figure 4.1: Layout of the muon spectrometer.

(absorber) required to reduce the flux of hadrons, measurement of low-p_t charmonia is possible only at small angles (i.e. at large rapidities) where muons are Lorentz boosted.

A resolution of 100 MeV/c^2 in the 10 GeV/c^2 dimuon invariant-mass region is needed to resolve the Υ, Υ' and Υ'' resonances. This requirement determined the bending strength of the spectrometer magnet as well as the spatial resolution of the muon tracking system. In addition, multiple scattering is minimized by a careful optimization of the absorber and very thin detector planes.

The tracking and trigger detectors of the spectrometer have to cope with the high particle multiplicity expected in heavy-ion collision at LHC energies and have therefore a very high granularity read-out. The spectrometer is equipped with a selective dimuon trigger system to match the maximum trigger rate handled by the DAQ [138].

4.2 Detector layout

The muon spectrometer is designed to detect muons in the polar angular range 171°–178°. This interval, a compromise between acceptance and detector cost, corresponds to the pseudo-rapidity range of $-4.0 \leq \eta \leq -2.5$.

The layout of the muon spectrometer is shown in figures 4.1 and 4.2. The spectrometer consists of the following components: a passive front absorber to absorb hadrons and photons from the interaction vertex; a high-granularity tracking system of 10 detection planes; a large dipole

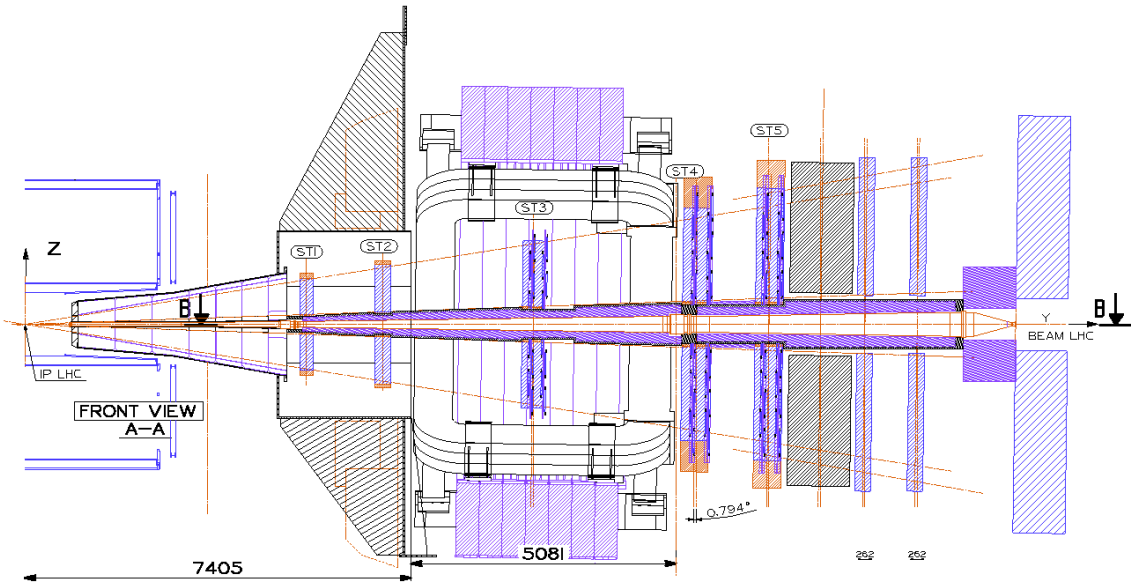

Figure 4.2: Muon spectrometer longitudinal section; according to the adopted numbering scheme station 1 (ST1) is the closest to the central barrel.

magnet; a passive muon-filter wall, followed by four planes of trigger chambers; an inner beam shield to protect the chambers from primary and secondary particles produced at large rapidities.

The main challenge for the muon spectrometer results from the high particle multiplicity per event rather than from the event rate, which is modest. Great care was taken both in the design of the absorbers (which have to provide strong absorption of the hadron flux coming from the interaction vertex) and of the detectors (which must be able to sustain the remaining high multiplicity). To optimize the spectrometer layout, simulations with FLUKA [139], C95 [140] and GEANT3 [141] were carried out. The particle yields predicted by the HIJING [142] event generator and multiplied by an extra (safety) factor of two were used as input. The main parameters of the muon spectrometer are summarised in table 4.1 and details on the dipole magnet are given in section 2.3.2 It is important to note that the muon spectrometer relies on the V0 detector as a fast interaction trigger to make the system more robust against background from beam-gas interactions in particular during the proton-proton run at nominal beam intensity [143]. A High-Level Trigger (HLT) for dimuons will reduce, by a factor four to five, the need in bandwidth and data storage.

4.3 Absorbers

The front absorber, whose length is 4.13 m ($\sim$10 $\lambda_{\rm int}$, $\sim$60 X_0), is located inside the solenoid magnet. The fiducial volume of the absorber is made predominantly out of carbon and concrete to limit small-angle scattering and energy loss by traversing muons. At the same time, the front absorber is designed to protect other ALICE detectors from secondaries produced within the absorbing material itself [144]. The spectrometer is shielded throughout its length by a dense absorber tube surrounding the beam pipe. The tube (beam shield) is made of tungsten, lead and stainless steel. It has a conical geometry to reduce background particle interaction along the length of the spectrometer. While the front absorber and the beam shield are sufficient to protect the tracking chambers,

2008 JINST 3 S08002

Table 4.1: Summary of the main characteristics of the muon spectrometer.

Muon detection	
Polar, azimuthal angle coverage	$171^\circ \leq \theta \leq 178^\circ$, 360°
Minimum muon momentum	$4\,\mathrm{GeV}/c$
Pseudo-rapidity coverage	$-4.0 < \eta < -2.5$
Front absorber	
Longitudinal position (from IP)	$-5030\,\mathrm{mm} \leq z \leq -900\,\mathrm{mm}$
Total thickness (materials)	($\sim$10 λ_{int}, $\sim$60 X_0) (carbon-concrete–steel)
Dipole magnet	
Nominal magnetic field, field integral	0.67 T, 3 T m
Free gap between poles	2.972–3.956 m
Overall magnet length	4.97 m
Longitudinal position (from IP)	$-z = 9.94\,\mathrm{m}$ (centre of the dipole coils)
Tracking chambers	
No. of stations, no. of planes per station	5, 2
Longitudinal position of stations	$-z = 5\,357, 6\,860, 9\,830, 12\,920, 14\,221\,\mathrm{mm}$
Anode-cathode gap (equal to wire pitch)	2.1 mm for st. 1; 2.5 mm for st. 2–5
Gas mixture	$80\,\%\mathrm{Ar}/20\,\%\mathrm{CO_2}$
Pad size st. 1 (bending plane)	$4.2 \times 6.3,\ 4.2 \times 12.6,\ 4.2 \times 25.2\,\mathrm{mm}^2$
Pad size st. 2 (bending plane)	$5 \times 7.5,\ 5 \times 15,\ 5 \times 30\,\mathrm{mm}^2$
Pad size st. 3, 4 and 5 (bending plane)	$5 \times 25,\ 5 \times 50,\ 5 \times 100\,\mathrm{mm}^2$
Max. hit dens. st. 1–5 (central Pb-Pb $\times 2$)	$5.0, 2.1, 0.7, 0.5, 0.6 \cdot 10^{-2}\,\mathrm{hits/cm}^2$
Spatial resolution (bending plane)	$\simeq 70\,\mu\mathrm{m}$
Tracking electronics	
Total no. of FEE channels	1.08×10^6
Shaping amplifier peaking time	$1.2\,\mu\mathrm{s}$
Trigger chambers	
No. of stations, no. of planes per station	2, 2
Longitudinal position of stations	$-z = 16\,120, 17\,120\,\mathrm{mm}$
Total no. of RPCs, total active surface	72, $\sim 140\,\mathrm{m}^2$
Gas gap	single, 2 mm
Electrode material and resistivity	Bakelite$^{\mathrm{TM}}$, $\rho = 2$–$8 \times 10^9\,\Omega\,\mathrm{cm}$
Gas mixture	$\mathrm{Ar/C_2H_2F_4/i\text{-}buthane/SF_6}$ (50.5/41.3/7.2/1)
Pitch of readout strips (bending plane)	10.6, 21.2, 42.5 mm (for trigger st. 1)
Max. strip occupancy bend. (non bend.) plane	3%(10%) in central Pb-Pb
Maximum hit rate on RPCs	3 (40) Hz/cm^2 in Pb-Pb (Ar-Ar)
Trigger electronics	
Total no. of FEE channels	2.1×10^4
No. of local trigger cards	$234 + 8$

additional protection is needed for the trigger chambers. For this reason the muon filter, i.e. an iron wall 1.2 m thick ($\sim$7.2 $\lambda_{\rm int}$), is placed after the last tracking chamber, in front of the first trigger chamber. The front absorber and muon filter stop muons with momentum less than 4 GeV/c.

4.4 Tracking system

Tracking chambers. The tracking chambers were designed to achieve a spatial resolution of about 100 μm, necessary for an invariant-mass resolution of the order of 100 MeV/c^2 at the Υ mass [145, 146]. In addition they can operate at the maximum hit density of about 5×10^{-2} cm^{-2} expected in central Pb-Pb collisions, where a few hundred particles are expected to hit the muon chambers. The tracking system covers a total area of about 100 m^2. All these requirements were fulfilled by the use of cathode pad chambers. They are arranged in five stations: two are placed before, one inside and two after the dipole magnet. Each station is made of two chamber planes. Each chamber has two cathode planes, which are both read out to provide two-dimensional hit information.[1] The first station is located right behind the absorber to measure the exit points of the muons as precisely as possible. To keep the occupancy at about 5%, a fine-granularity segmentation of the readout pads is needed. For instance, pads as small as 4.2×6.3 mm^2 were used for the region of the first station close to the beam pipe, where the highest multiplicity is expected. Since the hit density decreases with the distance from the beam, larger pads are used at larger radii, keeping the total number of channels at about one million.

Multiple scattering of the muons in the chambers is minimized by using composite materials (e.g. carbon fibre). The chamber thickness corresponds to about 0.03 X_0. Because of the different size of the stations, (ranging from few square metres for station 1 to more than 30 m^2 for station 5) two different designs were adopted. The first two stations are based on a quadrant structure [149], with the readout electronics distributed on their surface (see figure 4.3). For the other stations, a slat architecture, was chosen (see figure 4.4). The maximum size of the slat is 40 $\times$ 280 cm^2 and the electronics is implemented on the side of the slats. The slats and the quadrants overlap to avoid dead zones on the detector.

Extensive tests on several prototypes and on pre-production tracking chambers have shown that these detectors achieve the required performances [150, 151]. In particular, space resolutions of the order of 70 μm were measured.

Geometry monitoring system. The alignment of the spectrometer tracking chambers is crucial in order to achieve the required invariant-mass resolution of 100 MeV/c^2 at the Υ mass. Dedicated runs without magnetic field will be carried out at the beginning of each data taking period in order to align the ten tracking chambers with straight muon tracks, thus determining the initial geometry of the system. The displacements and deformations of the tracking chambers with respect to the initial geometry (due to different reasons, including switching on the magnetic field) will be measured and recorded during data taking by the Geometry Monitoring System (GMS). The requirement is to monitor the position of all the tracking chambers with a resolution better than 40 μm.

[1] Additional information about the clusterizer and tracking algorithms of the tracking system can be found in references [147, 148]

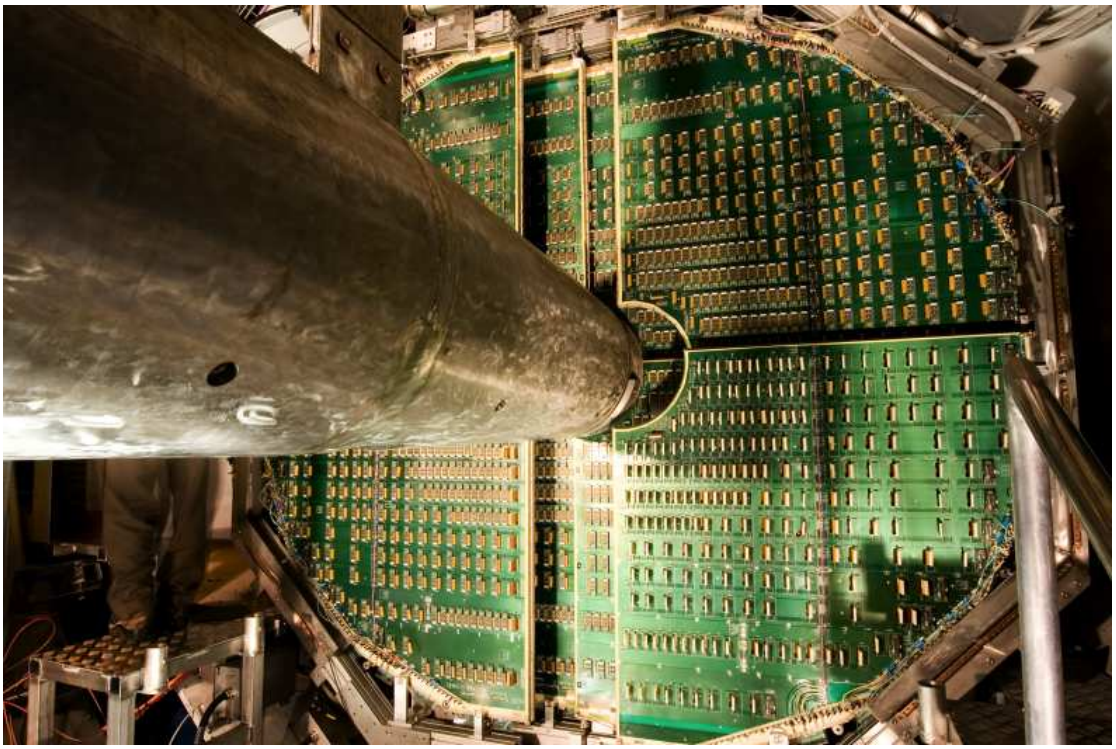

Figure 4.3: Layout of station 2 of tracking system. Readout electronics is distributed on the surface of a quadrant structure.

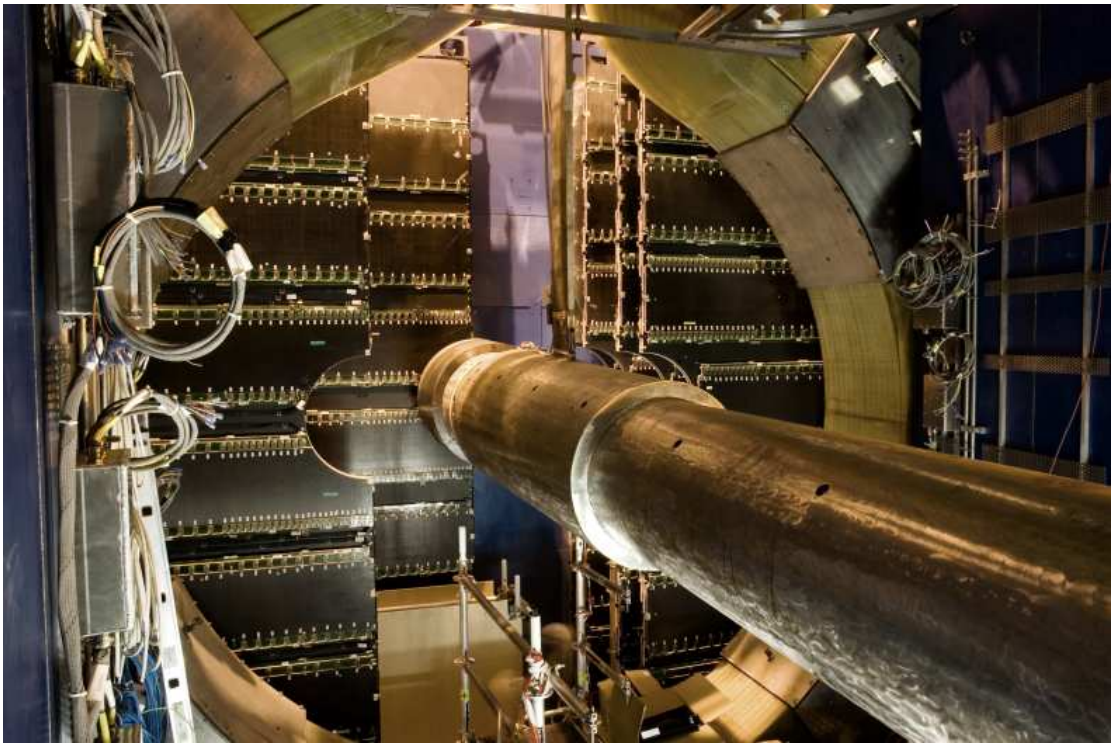

Figure 4.4: Layout of stations 4 and 5 of tracking system.

The GMS is an array of 460 optical sensors which are installed on platforms placed at each corner of the tracking chambers. Two different types of optical devices were adopted: the BCAM and the Proximity [152]. A detailed description of these devices can be found in [153]. In both cases, the image of an object is projected on a CCD sensor through a lens. The analysis of the recorded image provides a measurement of the displacement. The most relevant difference between the two systems is represented by the object (i.e. the light source) used. For the BCAM, which is a long-range system, the object is a pair of point-like LEDs, while it is a coded mask for the Proximity, which is used for small distances.

The GMS consists of three parts. The first one is the Longitudinal Monitoring System (LMS). Its role is to monitor the relative positions between the chamber planes. It is composed of BCAM lines linking two neighbouring stations, and Proximity lines linking the two chambers of each station. The second part is the Transverse Monitoring System (TMS). It monitors the flatness of the chamber support planes and is made of BCAM optical lines. Finally, the last part of the system is represented by the External Monitoring System (EMS). It is composed of eight BCAM lines linking the last chamber to the cavern walls to monitor the displacement of the whole spectrometer.

A complete simulation of the full system, including environment effects, was performed to evaluate the overall GMS performance [154]. The performance of a part of the system was studied in a laboratory test, with a full-scale mock-up of three half-planes of chambers 6,7 and 8. The test demonstrated that the GMS is able to measure transverse displacements from the initial position with an accuracy of 7 μm [155]. In this test, the effects of thermal gradients in the space between the chambers were investigated as well. When gradients similar to the ones expected in ALICE are generated, the measured resolution on transverse displacement turns out to be 23 μm. Such a value is well within specifications, including some safety margin.

Tracking electronics. The design of the electronics of the tracking system was driven by two main requirements: to read about one million channels up to a rate of the order of kHz and to achieve a space resolution of the tracking chambers of at least 100 μm. The electronics chain is divided in three parts: the front-end boards, called MANU (MAnas NUmérique), the readout system, called CROCUS (Cluster Read Out Concentrator Unit System) and the interface with the general ALICE trigger, called TCI (Trigger Crocus Interface) [156].

Great care was taken in the design of the front-end electronics and boards to achieve a noise as low as $\sim$1000 e, keeping at the same time the material budget as low as possible to minimize multiple scattering [12]. The front-end electronics is based, for all the tracking stations, on a 16-channel chip called MANAS (Multiplexed ANALogic Signal processor) including the following functionalities: charge amplifier, filter, shaper, and track & hold. The digitization of the signal is done on board. The channels of four of these chips are fed into a 12-bit ADCs, read out by the Muon Arm Readout Chip (MARC). This allows communication with the readout and performs zero suppression. This chain is mounted on front-end boards (MANUs). About 17 000 MANU cards are necessary to treat the 1.08 millions channels of the tracking system. Since the gain of each channel has to be precisely known to achieve the required space resolution, the parameters of each channel are checked just after the assembly of the boards. They will be controlled in periodic calibration runs during the data taking and stored for use in offline track reconstruction.

2008 JINST 3 S08002

The PATCH (Protocol for ALICE Tracking Chambers) buses provide the connection between the MANUs and the CROCUS crate. Each chamber is read out by two CROCUS, leading to a total number of 20 CROCUS. During the acquisition phase, the main tasks of the CROCUS are to concentrate and to format the data from the chambers, to transfer them to the DAQ and to dispatch the trigger signals. These crates also allow the control of the FEE and of the calibration processes. All these tasks are carried out in the CROCUS through a DSP and FPGA farm. Each CROCUS crate houses five frontal (FRT) data readout boards, which perform the first data concentration stage. Each FRT drives up to 10 PATCH buses and collects the data sent by the MANUs. The data from the FRTs are transferred to the data concentrator (CRT) board where they are encapsulated and then sent to the DAQ. So, a CROCUS is able to read up to 50 PATCH buses with a chamber occupancy up to 5% and with rates of the order of kHz.

The trigger signals, coming from the Central Trigger Processor (CTP), are distributed to the FEE through the CROCUS by the TCI. The main goals of the TCI are to decode the trigger signal, to generate the L1 reject in the FFT board (Frontal Fan-out Trigger) and to manage the busy signals of all the CROCUS crates. All these signals are sent to the twenty CROCUS via five FTD (Frontal Trigger Dispatching) cards.

All the components of the muon tracking electronics were intensively tested in laboratory, with beams and with cosmic rays [157–159]. In addition, radiation tests were successfully carried out. The FEE was tested with a proton beam [160] at a radiation level exceeding that for 10 years of ALICE running time by a factor of two. The CROCUS was tested using a neutron source. This test has shown that the number of SEU (Single Event Upset) in the worst case (first tracking station) will not exceed one SEU every two hours of data taking [161]. These performances fully satisfy the requirements of ALICE.

4.5 Trigger system

General considerations. In central Pb-Pb collisions, about eight low-p_t muons from π and K decays are expected to be detected per event in the spectrometer. To reduce to an acceptable level the probability of triggering on events where these low-p_t muons are not accompanied by the high-p_t ones emitted in the decay of heavy quarkonia (or in the semi-leptonic decay of open charm and beauty), a p_t cut has to be applied at the trigger level on each individual muon [162]. Two programmable cuts (low-p_t and high-p_t cuts), are performed in parallel by the trigger electronics [163]. The values of the p_t thresholds can range from $\sim$0.5 to $\sim$2 GeV/c. The following six trigger signals are delivered to the ALICE Central Trigger Processor (CTP), less than 800 ns after interaction, at 40 MHz frequency: at least one single muon track above low- (high-) p_t cut; at least two unlike-sign muon tracks, each of them above low- (high-) p_t cut; at least two like-sign muon tracks, each of them above low- (high-) p_t cut.

The threshold for the low-p_t and high-p_t cuts represents a compromise between background rejection and signal detection efficiency in the mass regions of the J/ψ and Υ resonances, respectively.

2008 JINST 3 S08002

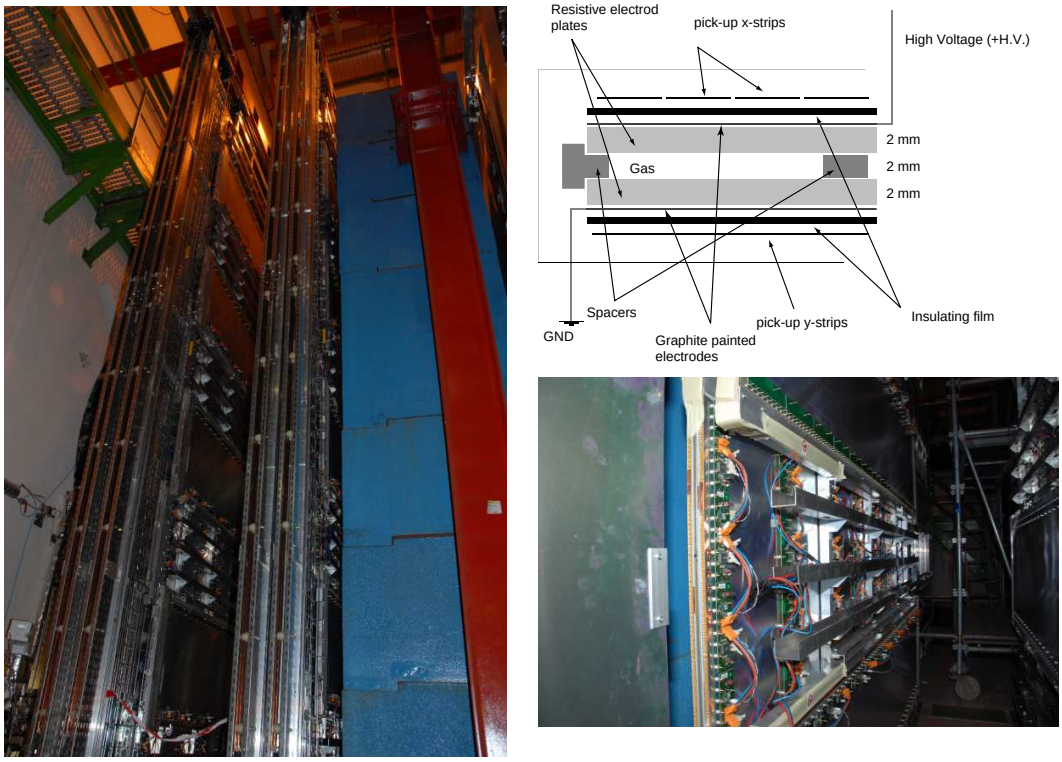

Figure 4.5: Left: view of the two trigger stations sitting behind the muon filter. Right-top: schematic view of an RPC cross section. Right-bottom: an individual RPC module equipped with the Front-End Electronics.

Trigger detector. To perform the p_t selection, a position-sensitive trigger detector with space resolution better than 1 cm is required. This resolution is achieved by Resistive Plate Chambers (RPCs) operated in streamer mode [164]. The trigger system consists of four RPC planes arranged in two stations, one metre apart from each other, placed behind the muon filter. Each plane consists of 18 RPC modules and the typical size of a module is about $70 \times 300\,\mathrm{cm}^2$, corresponding to a total active area of about $140\,\mathrm{m}^2$ [165]. The RPC electrodes are made of low-resistivity Bakelite ($\rho \sim 3 \times 10^9$ Ωcm), to attain the needed rate capability (maximum expected value about 40 Hz/cm^2 for Ar-Ar high-luminosity runs). To improve the smoothness of the electrode surface, these are coated with linseed oil. The (x,y) coordinates of the RPC hits are read out by segmented strips with pitch and length increasing with their distance from the beam axis.

Extensive tests were carried out to study the long-term behaviour of small-sized RPC prototypes operated in streamer mode. It was shown that RPCs are able to tolerate several ALICE years of data taking with heavy-ion beams [166]. It is worth noting that the detectors will take data for different colliding systems, resulting in a wide range of working conditions and requirements, in particular concerning position resolution and detector lifetime. The possibility of working in avalanche mode with the same front-end electronics was investigated in several beam and ageing tests [167] showing that this mode of operation is well suited for pp runs, where the requirements on the detector lifetime are more severe than in heavy-ion runs.

An overall view of the two trigger stations mounted at their final location is shown in figure 4.5. In the same figure an individual RPC module is shown as well.

2008 JINST 3 S08002

Trigger electronics. The RPCs are equipped with dual-threshold front-end discriminators [168] (ADULT), which are adapted to the timing properties of the detector and reach the necessary time resolution (1–2 ns) for the identification of the bunch crossing. From the discriminators, the signals are sent to the trigger electronics based on programmable circuits working in pipeline mode at 40 MHz. The trigger electronics is organized in 3 levels: local, regional and global. The local trigger algorithm of each local board searches for a single track pointing approximately back to the primary interaction vertex, using the information of the four RPC detector planes. Hits in at least 3 detector planes out of 4 are required to define a track, both in the bending and non-bending plane. The non-bending plane algorithm is very effective for background rejection. In the bending plane, the track deviation relative to a particle with infinite momentum is computed. Subsequent cuts on this deviation, performed by means of on-board look-up tables, allow delivering the low- and high-p_{t} trigger signals on single muons. Finally, the regional and the global levels gather the signals of all local boards and deliver the single muon, like-sign and unlike-sign dimuon triggers of the whole detector. The initial information from the detectors as well as the information at various stages of the local, regional and global algorithms are stored for readout in the corresponding boards.

2008 JINST 3 S08002